Supporting Information of

Density Functional Theory Study of Magnetic Properties of 2D Ferromagnetic Semiconductor $CrCl_{3-x}Br_x$ (x= 1-3) Monolayers

Hua Chen[a,1], Xu-li Wang[a,1], Hui-min Guo[a], Bing Wang[b,†], Jin Lv[a,*]and Hai-Shun Wu[a,*]

Calculation method of magnetic anisotropy energy (MAE)

MAE usually contains two main terms: magneto crystalline anisotropy energy resulting from spin-orbit coupling (SOC-MAE) and magnetic shape anisotropy energy induced by the dipole-dipole interaction (shape-MAE). The total MAE is the sum of SOC-MAE and shape-MAE. The SOC-MAE of $CrCl_{3-x}Br_x$ monolayers are calculated by using the force theorem,[1-3] in which the spin-orbit coupling (SOC) was considered based on the perturbation theory by Wang *et al*,[1] which can be expressed approximately in terms of angular momentum operators L_x and L_z as

$$MAE = \xi^2 \sum_{u,o;\alpha,\beta} (2\delta_{\alpha,\beta} - 1)\left[\frac{|\langle u,\alpha|L_z|o,\beta\rangle|^2 - |\langle u,\alpha|L_x|o,\beta\rangle|^2}{\varepsilon_{u,a} - \varepsilon_{o,\beta}}\right] \qquad (1)$$

where the ξ stands for the strength of SOC, $\varepsilon_{u,\alpha}$ and $\varepsilon_{o,\beta}$ are the energy levels of the unoccupied states (spin α) and occupied states (spin β), respectively. L_z and L_x are the angular-momentum operator with the magnetization along [001] and [100] directions, corresponding to transition $\triangle$m=0 and $\triangle$m=$\pm$1, respectively. Hence, in the same spin channel, the contribution from occupied and unoccupied states with identical

[1] Hua Chen and Xu-li Wang contributed equally to this study.

[a*] *Key Laboratory of Magnetic Molecules, Magnetic Information Materials Ministry of Education, School of Chemistry and Chemical Engineering, Shanxi Normal University, Taiyuan 030031, China.*
E-mail: lvjin_sxnu@163.com, wuhaishun@sxnu.edu.cn
[b†] *Institute for Computational Materials Science, School of Physics and Electronics, Henan University, Kaifeng 475004, China*
E-mail: wb@henu.edu.cn

(different) magnetic quantum number through the L_z (L_x) operator provides positive (negative) MAE, the opposite situation appears for different spin channels. The contributions to SOC-MAE can be analyzed from the hybridizations between different orbitals according to this definition. The shape-MAE, which originates from the magnetic dipole-dipole interaction, prefers to lie in the *xy* plane in the layered structure, which can be expressed as[4]

$$E^{dip-dip} = \frac{1\mu_0}{24\pi}\sum_{q\neq q'}^{N}\frac{1}{r_{qq'}^{3}}\left[M_q M_{q'} - \frac{3}{r_{qq'}^{2}}(M_q \cdot r_{qq'})(M_{q'} \cdot r_{qq'})\right] \qquad (2)$$

Where μ_0 is the permeability of vacuum, q is the atomic coordinate and M represents magnetic moment. The total MAEs are determined from an energy deviation between the total energies of two different magnetization directions, that is $MAE = E_{\parallel} - E_{\perp}$, where $E_{\parallel}$ and $E_{\perp}$ are the total energies with magnetization directions parallel or perpendicular to the plane of monolayers, respectively. Hence, the positive and negative values of the MAE represent the easy magnetization axis is perpendicular or parallel to the plane of the monolayers (We define these two MAE as the perpendicular magnetic anisotropy (PMA) and the in-plane magnetic anisotropy performance (IMA)).

(a) Various isomers of $CrCl_2Br$ monolayer

The bold lattice constant and energy of structure is the most stable structure.

symmetry	symmetry	symmetry
C_s	C_2	**C_2H**
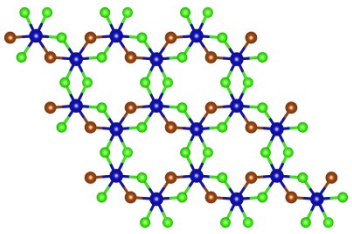	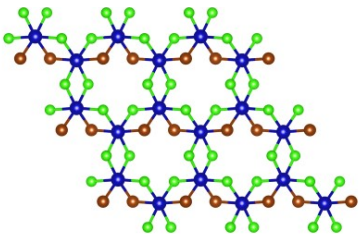	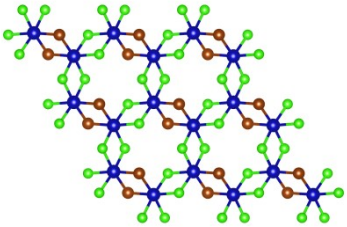
a=6.248 Å	a=6.242 Å	**a=6.246 Å**
E= -34.30699876 eV	E= -34.31717665 eV	**E= -34.31825483 eV**

(b) Various isomers of $CrClBr_2$ monolayer

The bold lattice constant and energy of structure is the most stable structure.

symmetry	symmetry	symmetry
C_2H	C_2	C_s
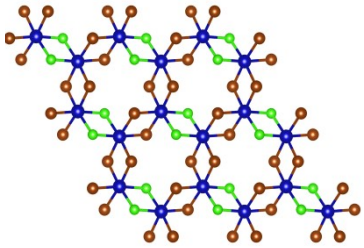	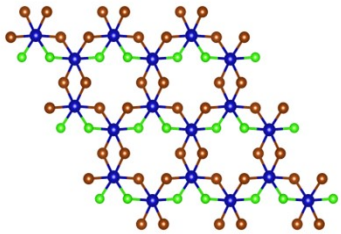	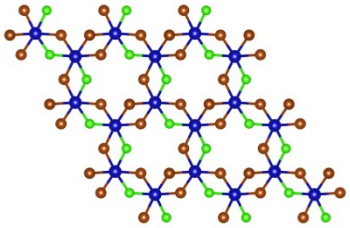
a=6.376 Å	a=6.372 Å	a=6.379 Å
E= -33.06719044 eV	E= -33.06480162 eV	E= -33.05650089 eV

Figure S1 Schematic diagram of various structures considered by $CrCl_2Br$ and $CrClBr_2$ monolayer.

Table S1 The magnetic ground state (G.S.), magnetic exchange coupling parameters $J_{1,2,3}$ (meV), magnetic anisotropy energy SOC-MAE (meV) and Curie temperature T_C (K), of the $CrCl_{3-x}Br_x$ monolayer under the different U_{eff}.

System		G.S.	J_1	J_2	J_3	SOC-MAE	Tc
$CrCl_3$	U=2.0 eV	FM	2.489	0.182	-0.057	0.043	27
	U=3.0 eV	**FM**	**2.625**	**0.174**	**-0.032**	**0.038**	**29**
	U=4.0 eV	FM	2.724	0.165	-0.029	0.035	29
$CrCl_2Br$	U=2.0 eV	FM	2.881	0.221	-0.230	0.076	32
	U=3.0eV	**FM**	**3.056**	**0.208**	**-0.222**	**0.055**	**34**
	U=4.0 eV	FM	3.222	0.206	-0.225	0.038	35
$CrClBr_2$	U=2.0 eV	FM	2.766	0.310	0.097	0.263	35
	U=3.0eV	**FM**	**3.194**	**0.292**	**-0.120**	**0.267**	**40**
	U=4.0 eV	FM	3.168	0.298	0.148	0.275	40
$CrBr_3$	U=2.0 eV	FM	3.137	0.350	-0.052	0.334	41
	U=3.0eV	**FM**	**3.403**	**0.340**	**-0.032**	**0.325**	**43**
	U=4.0 eV	FM	3.680	0.345	-0.014	0.325	47

Table S2 Optimized lattice constant a_0 (Å), the bond length of chromium and halogen atoms $d_{Cr\text{-}X}$ (Å), the distance of two chromium $d_{Cr\text{-}Cr}$(Å), and the bond angle $\theta_{Cr\text{-}X\text{-}Cr}$ (deg) of $CrCl_{3-x}Br_x$ monolayers.

System	a_0(Å)	$d_{Cr\text{-}X}$(Å)	$d_{Cr\text{-}Cr}$(Å)	$\theta_{Cr\text{-}X\text{-}Cr}$(deg)
$CrCl_3$	6.116	2.383	3.531	95.59
$CrCl_2Br$	6.246	2.392(Cl)	3.558(Cl)	96.14(Cl)
		2.533(Br)	3.705(Br)	93.99(Br)
$CrClBr_2$	6.376	2.397(Cl)	3.575(Cl)	96.46(Cl)
		2.541(Br)	3.735(Br)	94.54(Br)
$CrBr_3$	6.504	2.548	3.755	94.93

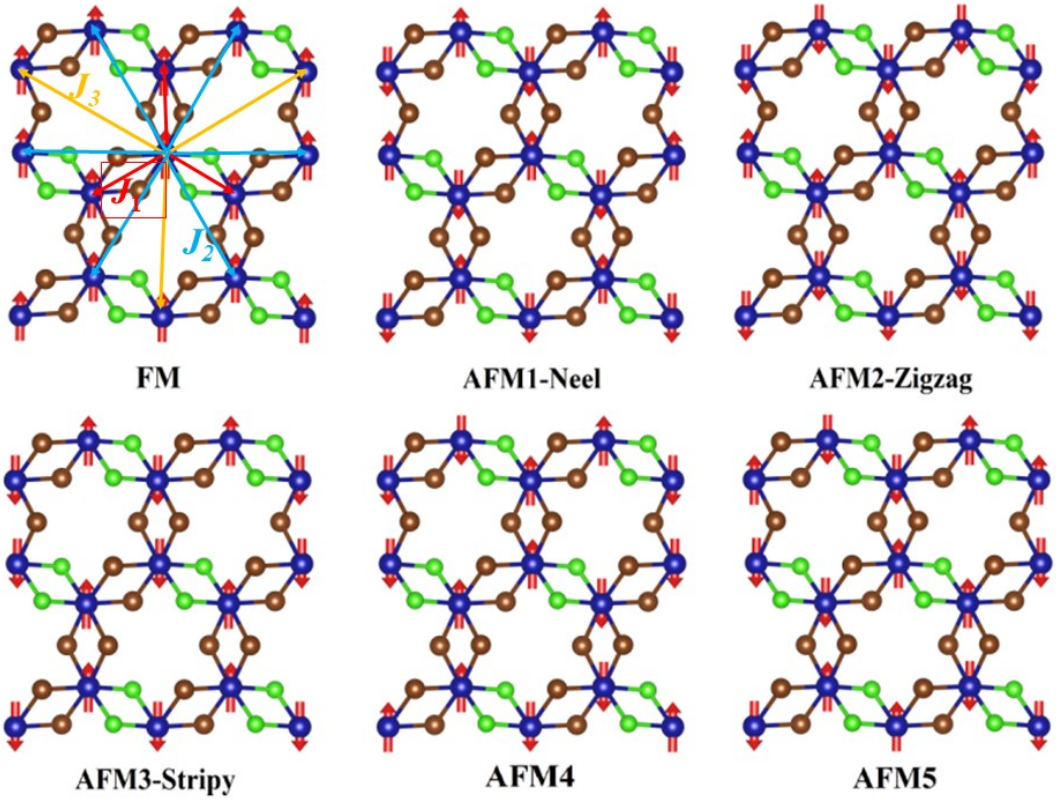

Figure S2 The possible magnetic configuration of $CrCl_2Br$ and $CrClBr_2$ monolayer and the sketch map of the magnetic exchange coupling parameters $J_{1,2,3}$. The red arrows represent the spin direction of Cr atoms.

Table S3 The energy bands characteristic parameter of $CrCl_{3-x}Br_x$ monolayer calculated using PBE+U and HSE06 functions.

system	PBE+U/eV			HSE06/eV		
	up	down	gap	up	down	gap
$CrCl_3$	2.34	4.17	2.34	3.74	5.31	3.74
$CrCl_2Br$	2.07	3.83	2.07	3.33	4.88	3.33
$CrClBr_2$	1.88	3.74	1.88	2.97	4.70	2.97
CrBr3	1.75	3.70	1.75	2.80	4.64	2.80

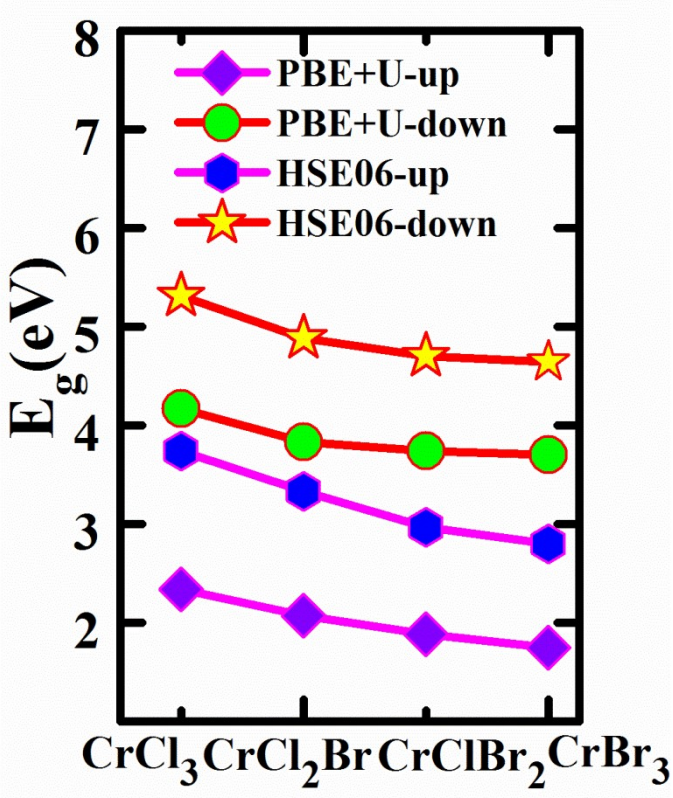

Figure S3 The change curve of spin-up and spin-down band gap under different methods.

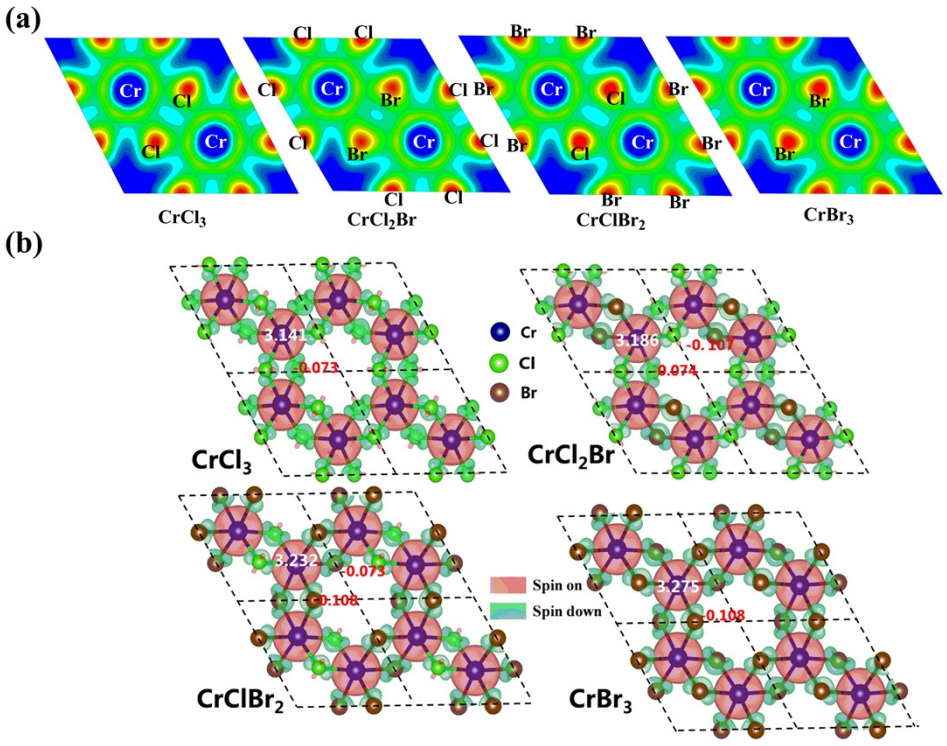

Figure S4 (a) The Electron Localization Function (ELF)of $CrCl_{3-x}Br_x$ monolayer. The blue color shows the electron dissipation, and the red color shows the electron accumulation. (b) The spin polarized charge density for $CrCl_3$, $CrCl_2Br$, $CrClBr_2$ and $CrBr_3$. The red and green areas indicate spin up and spin down.

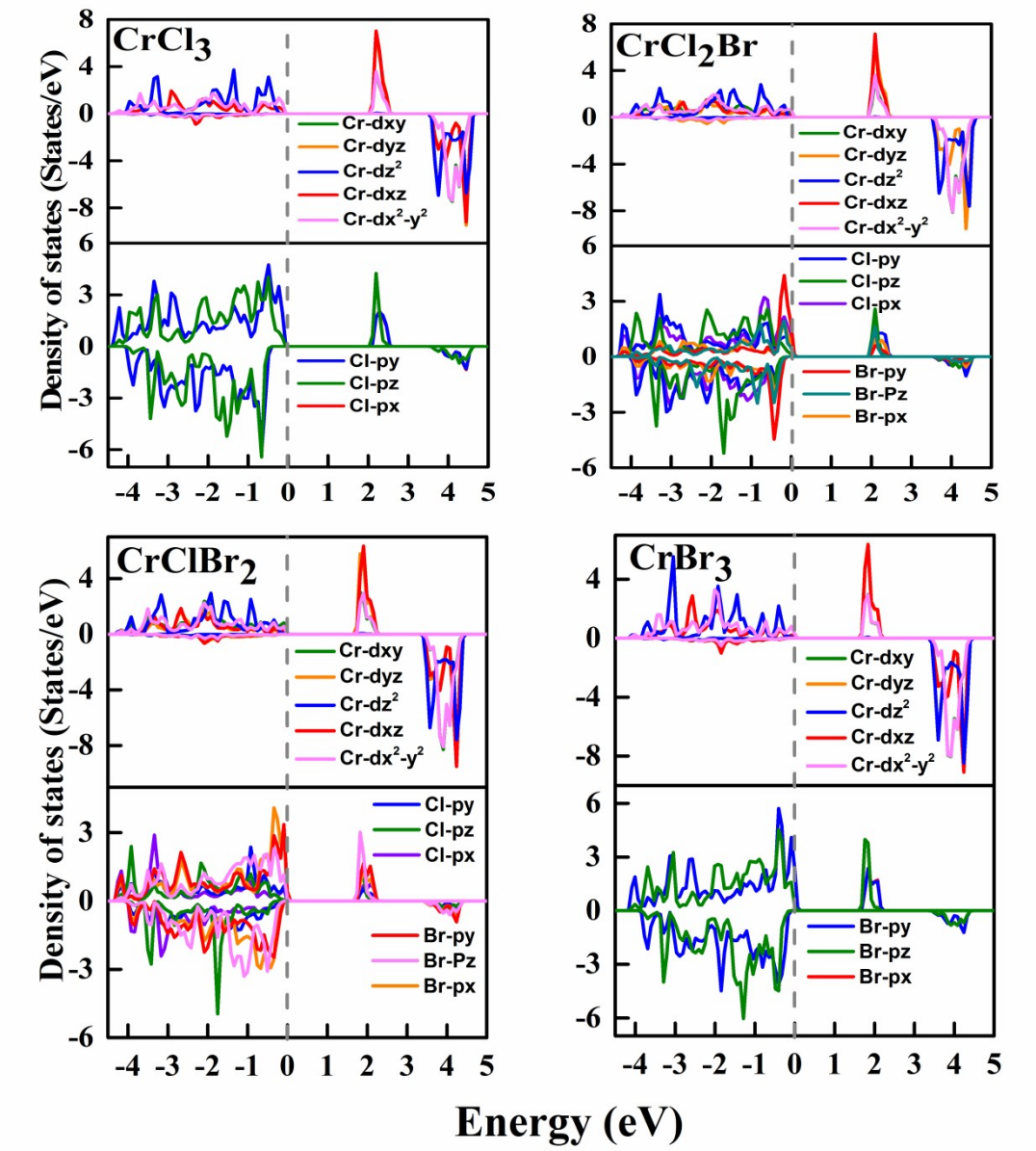

Figure S5 The projected DOSs of d and p orbitals of Cr and X atoms for $CrCl_3$, $CrCl_2Br$, $CrClBr_2$, and $CrBr_3$ monolayer.

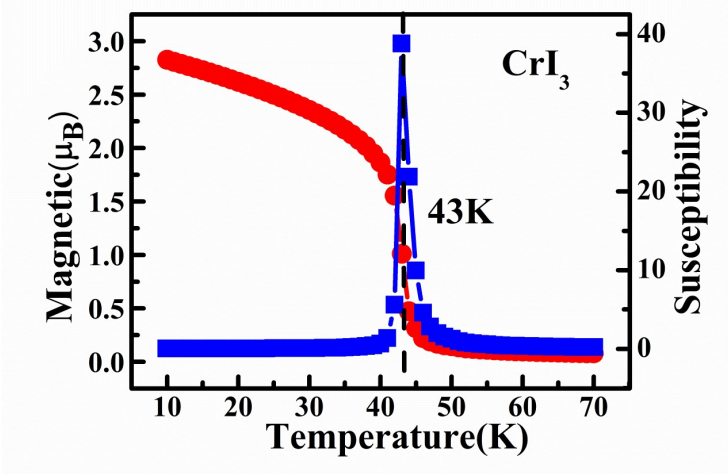

Figure S6 The Curie temperature of CrI_3monolayer calculated by Monte Carlo method. The red and blue curve are denoted to magnetic moments and susceptibility as a function of temperature. The nearest exchange-coupling parameter J_1 is 2.94 meV and magnetic anisotropy energy $(MAE = E_x - E_z)$ is 744 μeV/Cr. The calculated T_c of CrI_3 monolayer is 43 K. These values are consistent with previous works.[5]

Detail of Monte Carlo (MC) simulations

The Monte Carlo algorithm adopted by us is the classic Monte Carlo simulation software package provided by Professor Wang Jinlan's research group of Southeast University, which is a general multidimensional Monte Carlo simulation program based on classical Heisenberg model. And backward compatible with the simulation of Ising model. And the specific details can be briefly summarized as: "Based on the MC scheme, the spins on all magnetic sites flip randomly, by using a 2D 50 × 50×1 supercell to perform 10^5 MC steps for each temperature, the exact solution of the spin-Hamiltonian can be provided, and finally the T_C can then be estimated by locating the peak position of the magnetic susceptibility and the magnetic moment change curve."[6]

Table S4 The Tc (K) of $CrCl_{3-x}Br_x$ monolayer after the inclusion of J_2 and J_3.

System	Tc/J_1	Tc/J_1+J_2	$Tc/J_1+J_2+J_3$
$CrCl_3$	29	35	35
$CrCl_2Br$	34	45	40
$CrClBr_2$	40	53	50
$CrBr_3$	43	59	58

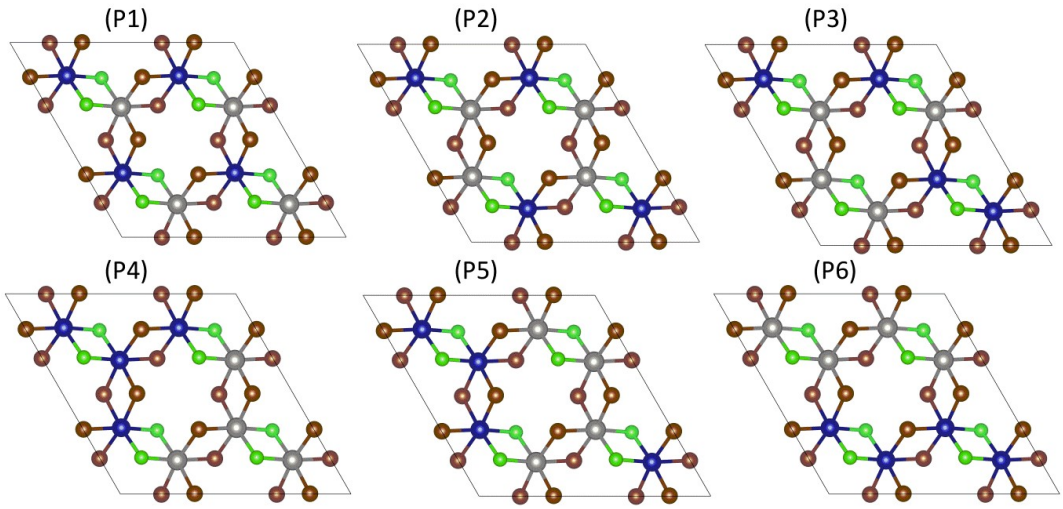

Figure S7 Considered six different configurations in the 2×2×1 supercell. The blue, green, brown, and gray balls represent Cr, Cl, Br, and W atoms, respectively.

Table S5 The energy of the different alloyed configurations (P1-P6) of the $CrCl_{3-x}Br_x$-W monolayer.

System	P1/meV	P2/meV	P3/meV	P4/meV	P5/meV	P6/meV
$CrWCl_6$	**-152.271**	-151.975	-151.970	-152.210	-151.818	-151.657
$CrWCl_4Br_2$	**-147.166**	-146.878	-146.888	-146.737	-146.743	-146.599
$CrWCl_2Br_4$	**-142.130**	-141.879	-141.863	-141.730	-141.734	-141.589
$CrWBr_6$	**-137.162**	-136.924	-136.921	-136.794	-136.800	-136.672

Table S6 Optimized lattice constant a_0 (Å), the bond length of chromium and halogen atoms d_{Cr-X} (Å) and two chromium d_{Cr-Cr} (Å), and the bond angle θ_{Cr-X-W} (deg) of $CrCl_{3-x}Br_x$-W monolayer.

System	a_0(Å)	d_{Cr-X}(Å)	d_{W-X}(Å)	d_{Cr-W}(Å)	$\theta_{Cr-X-Cr}$(deg)
$CrWCl_6$	6.279	2.443	2.428	3.625	96.17
$CrWCl_4Br_2$	6.400	2.460(Cl)	2.431(Cl)	3.657(Cl)	96.62(Cl)
		2.582(Br)	2.575(Br)	3.775(Br)	94.12(Br)
$CrWCl_2Br_4$	6.510	2.459(Cl)	2.437(Cl)	3.672(Cl)	97.18(Cl)
		2.591(Br)	2.581(Br)	3.803(Br)	94.59(Br)
$CrWBr_6$	6.626	2.597	2.586	3.826	95.19

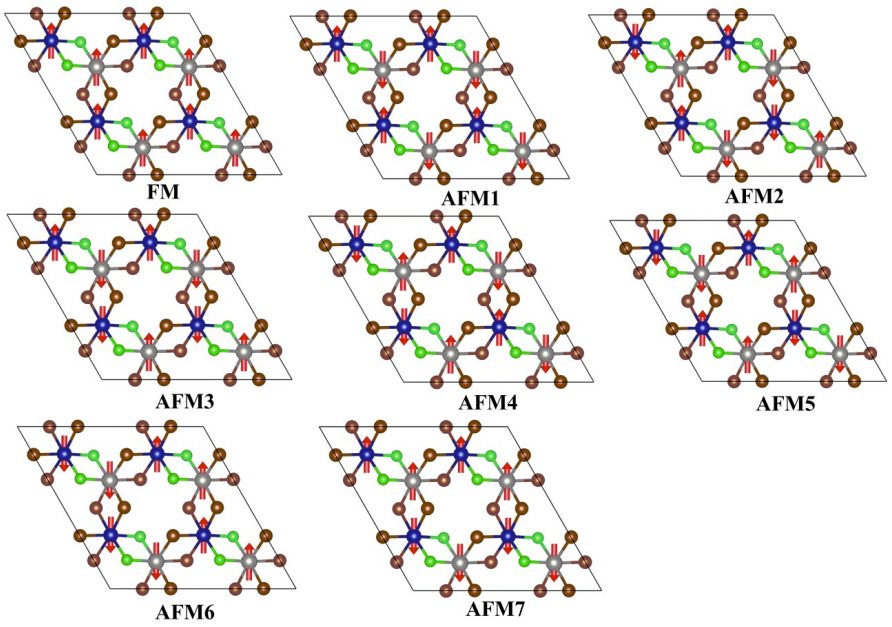

Figure S8 Considered possible magnetic configurations of $CrWCl_{3-x}Br_x$monolayer, including one FM and seven AFM.

Table S7 The magnetic ground state (G.S.), magnetic exchange energy differences ΔE_{ex} (E_{AFM}-E_{FM}), magnetic exchange coupling parameters $J_{1,2,3}$ (meV) and magnetic anisotropy energy (MAE) of the $CrCl_{3-x}Br_x$-W monolayer.

System	G.S.	ΔE_{ex}/ meV	J_1/meV	J_2/meV	J_3/meV	MAE/unit/ meV
$CrWCl_6$	FM	148.196	1.371	1.614	1.373	2.477
$CrWCl_4Br_2$	FM	243.419	9.522	-1.146	2.146	2.762
$CrWCl_2Br_4$	FM	223.897	15.470	-2.238	1.973	3.045
$CrWBr_6$	FM	244.592	17.208	-0.733	-0.229	2.542

References

1 X. Wang, R. W., D. Wang and A. J. Freeman, Phys. Rev. B, 1996, **54**, 61-64.

2 J. Hu and R. Q. Wu, Phys. Rev. Lett., 2013, **110**, 097202.

3 J. Zhang, B, Yang, H. Zheng, X. Han and Y. Yan, Phys. Chem. Chem. Phys., 2017, **19**, 24341-24347.

4 K. Yang, G. Wang, L. Liu, D. Lu and H. Wu, *Phys. Rev. B.*, 2021, **104**, 144416.

5 B. Huang, G. Clark, E. Navarro-Moratalla, D. R. Klein, R. Cheng, K. L. Seyler, D. Zhong, E. Schmidgall, M. A. McGuire, D. H. Cobden, W. Yao, D. Xiao, P. Jarillo-Herrero and X. D. Xu, Nature, 2017, **546**, 270-273.

6 Y. H. Zhang, B. Wang, Y. L. Guo, Q. Li and J. L. Wang, Comput. Mater. Sci., 2021, **197**, 110638.